

HOSTED BY



ELSEVIER

Contents lists available at ScienceDirect

Journal of King Saud University – Science

journal homepage: www.sciencedirect.com

Original article

Design of MEMS capacitive comb accelerometer with perforated proof mass for seismic applications

Ghada Ahmed Khouqeer^a, S. Suganthi^{b,1,*}, Nadyah Alanazi^c, Abdullah Alodhayb^{c,d}, Muthumareeswaran Muthuramamoorthy^{d,*}, Saravanan Pandiaraj^e^a Department of Physics, Imam Mohammad Ibn Saud Islamic University (IMSIU), Riyadh, Saudi Arabia^b Department of Electronics and Communication Engineering, Rajalakshmi Engineering College, Thandalam 602105, Tamilnadu, India^c Department of Physics and Astronomy, College of Science, King Saud University, Riyadh 11451, Saudi Arabia^d King Abdullah Institute for Nanotechnology, King Saud University, Riyadh 11451, Saudi Arabia^e Department of Self Development Skills, CFY Deanship, King Saud University, Riyadh, Saudi Arabia

ARTICLE INFO

Article history:

Received 4 October 2022

Revised 20 December 2022

Accepted 9 January 2023

Available online 20 January 2023

Keywords:

Environmental quantity

MEMS

Sensors

Accelerometer

Seismology

Perforated mass

Etch hole

Proof mass

ABSTRACT

Micro Electro Mechanical System (MEMS) sensors are characterized by their small size, but their performances exceed that of their macro-scale counterparts. The small size of MEMS devices and their integration with microelectronics proves a major advantage. In this paper, a design of MEMS capacitive comb accelerometer for seismology application using COMSOL Multiphysics platform is presented. A seismometer (also known as a seismograph) is a device that is used to measure and record the behavior of seismic waves. With this data, the location and measure of earthquakes can be detected. This seismic device has a large frequency band, compared to traditional geophones and seismographs. In this paper, a study to measure amplitudes and frequencies of vibrations is presented, and the results are analyzed and compared for perforated mass and solid proof mass. The effect of the size of etch hole for perforation is also studied. The displacement sensitivity and capacitive sensitivity of accelerometer are found to be $1.188 \times 10^{-9} \text{m/g}$ and $1.093 \times 10^{-21} \text{F}$, respectively.

© 2023 The Author(s). Published by Elsevier B.V. on behalf of King Saud University. This is an open access article under the CC BY license (<http://creativecommons.org/licenses/by/4.0/>).

1. Introduction

Micro-Electro-Mechanical Systems (MEMS) sensors encompass a wide range of applications in all domains. The MEMS devices or systems are able to control, actuate and sense on the micro scale, and produce responses on the macro scale. The use of MEMS devices for various applications has seen an increase over the last decades. Over the traditional methods, the MEMS sensors are preferred because of their reduced dimension and weight, better long-term endurance, and their ease of handling. An accelerometer is a sensor that measures the acceleration or simply the vibration of a

structure (Kavitha et al., 2016). Accelerometers can be used to determine the position and monitor the movement of the earth. It is done by converting a mechanical strain into an electrical signal (Xu et al., 2017). In addition, accelerometers accurately sense the change in inertia of automobiles and deploy the airbag within a fraction of a second. Other applications of the accelerometer are in aircraft and aviation industry for enhanced aerodynamic performance of turbines, compressors (Raaja-Bhaskaran et al., 2017). In military applications, micro accelerometers are used in distributed battlefield sensor net (DBSN) for accurate detection of targets. The integration of mechanical elements and electronic components reduces interference noise and avoids parasitic capacitances.

Accelerometers can be majorly classified as i) Piezoelectric ii) Piezoresistive and iii) Capacitive. Among these, the capacitive type is employed for seismology applications because of its high sensitivity, lower temperature coefficients, low power consumption, and excellent stability (Xu et al., 2017; Utz et al., 2018). Capacitive accelerometers with comb-drives *i.e.*, interdigitated electrodes are used in a variety of MEMS sensors for inertial applications (Scudero et al., 2018).

* Corresponding authors.

E-mail addresses: suganthi.s@rajalakshmi.edu.in (S. Suganthi), mramamoorthy@ksu.edu.sa (M. Muthuramamoorthy).

¹ Authors equally contributed to this work.

Peer review under responsibility of King Saud University.



Production and hosting by Elsevier

<https://doi.org/10.1016/j.jksus.2023.102560>

1018-3647/© 2023 The Author(s). Published by Elsevier B.V. on behalf of King Saud University. This is an open access article under the CC BY license (<http://creativecommons.org/licenses/by/4.0/>).

MEMS accelerometers do not need a fixed reference for the measurement, they are used for the measurement of linear motion, and vibration (Varanis et al., 2018). The measurement of seismic motion is important for a wide range of applications in geology, civil structure monitoring, etc (Qu et al., 2008; Zhang et al., 2019). Replacement of the conventional seismometers that require vacuum sealing and hence are relatively very bulky, COMSOL Multiphysics®, a powerful simulation platform is used in this paper. From modelling the geometry, adding materials, defining physics, studying, all these can be done, and the results produced are accurate and trustworthy.

The MEMS comb-drive capacitive accelerometer was developed by researcher for use in SHM and seismic monitoring (Kavitha et al., 2016). The IntelliSuite MEMS modelling tool was used to simulate a surface micromachined capacitance comb drive accelerometer model. This was designed specifically for Structural Health Monitoring (SHM) applications in which low-frequency accelerations with high resolution are necessary. A piezoelectric accelerometer was developed specifically for SHM applications. (Raaja-Bhaskaran et al., 2017). A simple analytical model for MEMS cantilever beam piezoelectric accelerometer and high sensitivity design for SHM is discussed. The accelerometers must work at a lower frequency spectrum while still having a high sensitivity and a low noise floor. The drawback in this design is that the stability and sensitivity of the sensor when compared to the capacitive accelerometer the performance is lower.

Authors also designed a MEMS capacitive accelerometer with high precision and bandwidth (Utz et al., 2018). A low noise readout-IC and a high-precision bulk micro-machined sensing element are used in this accelerometer. The comparisons of various systems literature as well as commercial products are provided by the authors. Researchers developed a MEMS seismometer and geophones (Hou et al., 2021). As opposed to conventional instruments, the design is based on a small-scale seismometer, which would achieve greater sensitivity with a wider frequency range (Chen et al., 2013; Sabato et al., 2016; Tilli et al., 2020). The major drawback of this design is the limited proof mass for sensing, which has resulted in thermodynamic self-noise, which may impair the sensitivity (Mougenot and Thorburn, 2004; van Bakel, 2013; Laine and Mougenot, 2014; Peng et al., 2017).

2. Working principle

This comb-type capacitive accelerometer used in this work senses the change in capacitance with respect to acceleration. When vibration is being experienced, the proof mass anchored by the spring displaces and can move the combs attached to it with the same rate equal to the vibrations it sensed (Gupta and Mukherjee, 2000; Zhang et al., 2019). As a result of this, the distance between the plates (d) decreases. The capacitance (C) is inversely proportional to the distance between the plates (d) as seen in equation (1).

$$C = \frac{\epsilon A}{d} \quad C = \frac{\epsilon A}{d} \quad (1)$$

Where ϵ is the relativity permittivity. This change in capacitance is measured in volts as per the equation (2).

$$C = \frac{Q}{V} \quad (2)$$

2.1. Design

2.1.1. Analytical design

The general analytical mass spring damper model of the accelerometer is as shown in (supplementary file) fig. S1:

The differential equation for the mechanical model is as follows:

$$M \frac{d^2x}{dt^2} + D \frac{dy}{dx} + Kx = Ma \quad (3)$$

Where, D is the damping coefficient, K is the spring constant, M is the proof mass, and ' a ' is the acceleration applied externally. To obtain the second order transfer function, we use the Laplace transformation (Lynch et al., 2003):

$$[Ms^2 + Ds + k]X(s) = MA(s) \quad (4)$$

$$\frac{X(s)}{A(s)} = \frac{M}{[Ms^2 + Ds + k]} \quad (5)$$

$$\frac{X(s)}{A(s)} = \frac{M}{[Ms^2 + Ds + k]} \quad (6)$$

$$TF = \frac{X(s)}{A(s)} = \frac{1}{s^2 + \frac{D}{M}s + \frac{k}{M}} \quad (7)$$

For damped mass spring system, the quality factor Q is given by

$$Q = \frac{\sqrt{Mk}}{D} = \frac{M\omega_r}{D} \quad (8)$$

Where ω_r is the resonant frequency which is given by:

$$\omega_r = \sqrt{\frac{K}{M}} \Rightarrow \omega_r^2 = \frac{K}{M} \quad (9)$$

At low frequency ($\omega \ll \omega_r$) we have

$$\frac{X}{A} \approx \frac{1}{\omega_r^2} \quad (10)$$

Thus, the sensitivity is inversely proportional to square of resonant frequency. Lower ω_r , higher the sensitivity. But it is limited by various factors (Trapani et al., 2012; Benmessaoud and Nasreddine, 2013) like mechanical shock resistance, Low spring constant, etc.

For the system, the inertial force is given as

$$F_{inertial} = Ma \quad (11)$$

From Hooke's law

$$F_{damping} = kx \quad (12)$$

Equating the two forces we find that the displacement is given as:

$$x = \frac{Ma}{k} \quad (13)$$

From the Fig. 1, the capacitance when no acceleration is applied is given by:

$$C_0 = \frac{\epsilon A}{d} \quad (14)$$

When acceleration is applied, the movement of fingers is opposite to that of the direction of acceleration applied, the capacitance changes. The left and right capacitances with respect to the plate are given as follows:

$$C_{left} = \frac{\epsilon A}{d+x} \text{ and } C_{right} = \frac{\epsilon A}{d-x} \quad (15)$$

where, x is the displacement of the proof mass, A is the overlap area between all the electrodes in sensing area, ϵ is permittivity of air, d is the capacitance gap.

The differential capacitance of the accelerometer is as

$$\Delta C = \frac{\epsilon A}{d+x} - \frac{\epsilon A}{d-x} \quad (16)$$

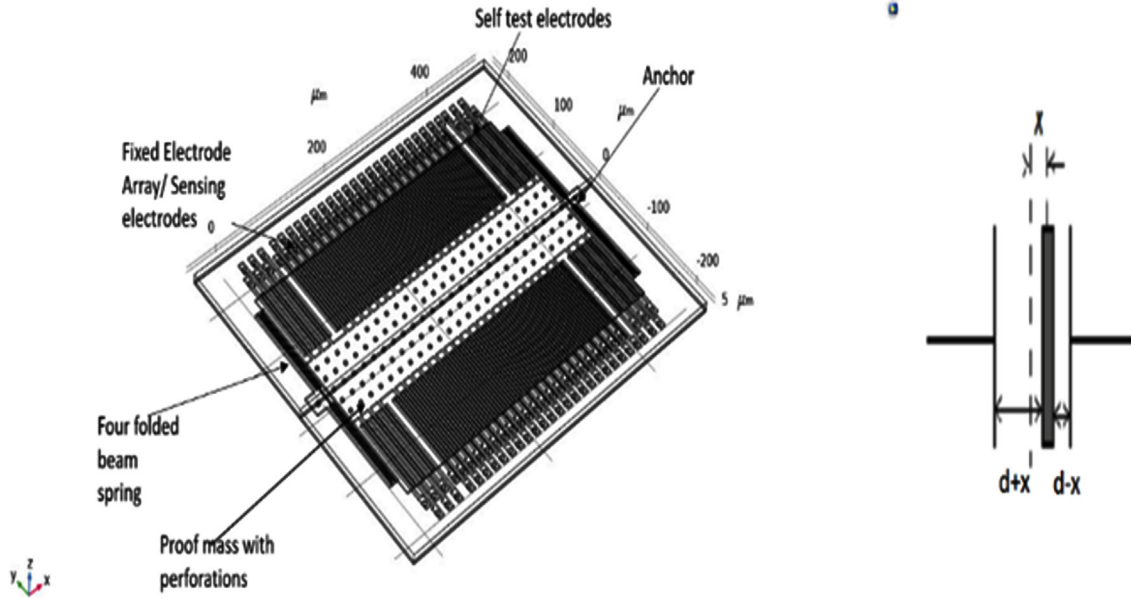


Fig. 1. Structure of the accelerometer.

$$\Delta C \approx \frac{2C_0x}{d} \quad (17)$$

From equations (14) and (17) we get

$$\Delta C \approx \frac{2C_0Ma}{kd} \quad (18)$$

It is observed that the change in capacitance is directly proportional to acceleration ($\Delta C \propto a$).

2.1.2. Mathematical analysis

The spring constant of the structure is given by

$$K_s = \frac{1}{2} \cdot E \cdot h \cdot \left(\frac{W_b}{L_b}\right)^3 \quad (19)$$

Where E is the young's modulus of polysilicon, h is the beam thickness, W_b is the beam-width, L_b is the length of the beam. For the proposed model it is calculated as 0.1567 N/m.

Due to the gap between the comb and the fingers, there occurs damping. The coefficient of damping can be given as follows:

$$D = N_f \times n_{eff} \times l_b \times \left(\frac{h}{d_0}\right)^3 \quad (20)$$

N_f is total sensing finger number, n_{eff} is the effective viscosity of air, and d_0 is capacitance gap.

2.1.3. Material used

Polysilicon is used for the proof mass, anchor, spring, and fingers in the proposed model. An air-box surrounds the entire polysilicon structure. The physics function called body load domain is used to apply an acceleration to this. The proof mass and its attached electrodes are at a floating potential whose value is determined by the position-dependent capacitance and the applied voltages on the fixed sense electrodes (Gonenli et al., 2011).

2.1.4. Geometry

The geometry is designed to the following specifications:

- The dimensions of proof mass ($L \times W$) are $448 \times 200 \mu\text{m}$.
- There are 12 Self-test fingers and 42 Sense fingers on each side.

- Each finger has a width of $4 \mu\text{m}$ and length of $114 \mu\text{m}$.
- The gap between the fingers is $1 \mu\text{m}$.
- For providing the perforations in the proof mass, it is etched to $4 \mu\text{m}$ size at a period of $18 \mu\text{m}$.
- The spring has (length \times width \times gap) of $(280 \times 2 \times 1) \mu\text{m}$.
- The spring is connected with the anchor of $17 \times 17 \mu\text{m}$ in size with radius of base $3 \mu\text{m}$.
- Short electrode has a length of $120 \mu\text{m}$ and long electrode has length of $140 \mu\text{m}$.
- The electrodes are attached with the pad of dimension $16 \mu\text{m} \times 8 \mu\text{m}$.
- The finger overlap length is $104 \mu\text{m}$. The total length is given by (length of proof mass + $2 \times$ Length of spring assembly).

2.1.5. Comparison with existing model

The geometrical parameters of the existing system (Kalaiselvi et al., 2020) and the proposed system is compared as shown in the (supplementary file) table s1.

Seismic applications require a high sensitivity accelerometer. Therefore, we need to increase sensitivity. As sensitivity is inversely proportional to the spring constant, it needs to be reduced. This can be done by making use of the folded beam structure (Xiong, 2005; Mistry et al., 2010; Zou et al., 2014).

2.1.6. Performance parameters

The following Table 1 shows the required parameter values for the design of seismic applications.

Table 1
Comparison of parameters with optimum value.

Parameter	Optimum value	Model value
Noise spectral density	below $1 \mu\text{g}/\sqrt{\text{Hz}}$	$14.97 \text{ ng}/\sqrt{\text{Hz}}$
Resolution	Below 10^{-6} ms^{-2}	10^{-9} ms^{-2}
Sensor linearity	Linear at low power	The output is linear
Resonant frequency	Between 10^5 and 10^3 Hz	z

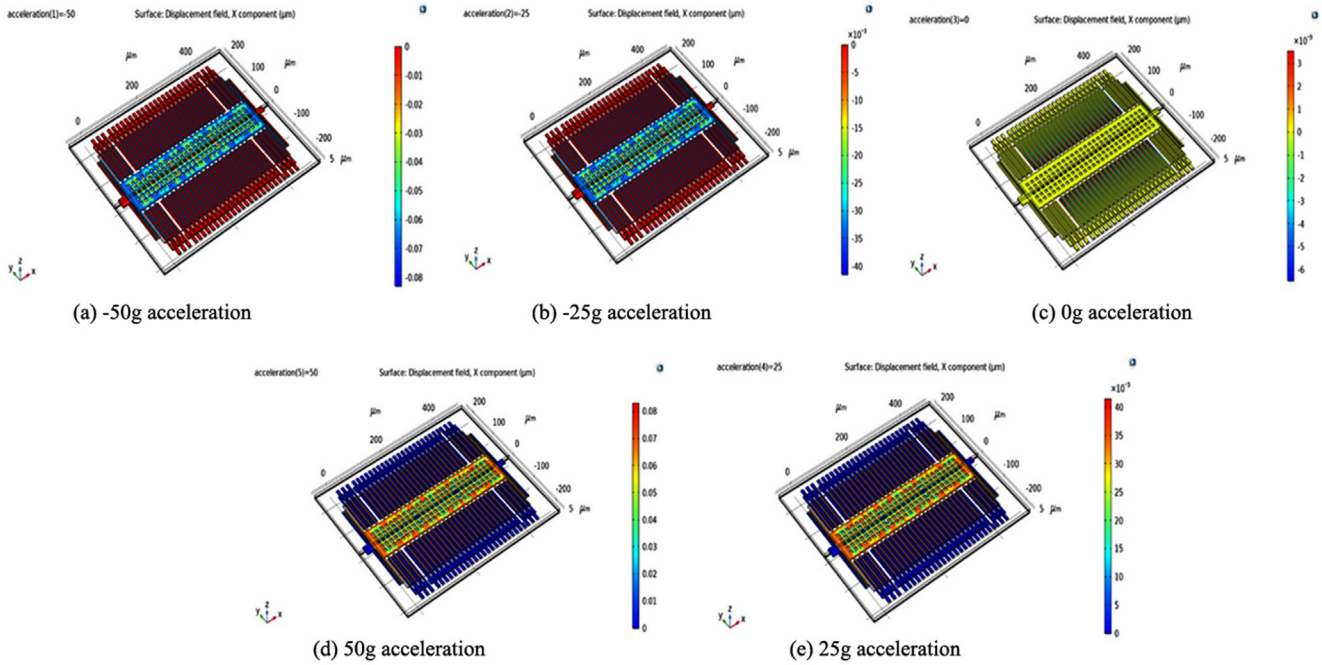


Fig. 2. Simulation result with perforated mass: Displacement field for X component for -50 g (fig. a); -25 g (fig. b); 0 g (fig. c); 25 g (fig. e) 50 g (fig. d) acceleration.

3. Results

3.1. Study i: With perforated mass $4[\mu\text{m}]$ Etching & $18[\mu\text{m}]$ period

By applying acceleration in the range -50 g to $+50$ g with 25 as step increment size, the change in the displacement occurring in the proof mass is analysed; the Fig. 2 depict the results.

3.2. Study II: Without perforated mass

By applying acceleration in the range -50 g to $+50$ g with 25 as step increment size, the result of the displacement occurring in the proof mass is analysed and the results depicts in Fig. 3.

As shown in Fig. 4, the set electrodes and the anchored spring bases shift very little. As anticipated, the springs have varying displacements along their length. In the actual unit, the potential at the fixed electrode is generated due to high frequency square wave that has opposite phase to that of the movable electrodes. These movable electrodes have a potential approximately equal to 50% of supply voltage.

The fixed self-test electrodes are applied with a potential which is equal to half of supply voltage. Due to the applied acceleration, the proof mass displaces, this induces a capacitive coupling between the electrodes attached to proof mass and the set electrodes. As a consequence, an alternating voltage is caused. The above configuration eliminates the electrostatic force between

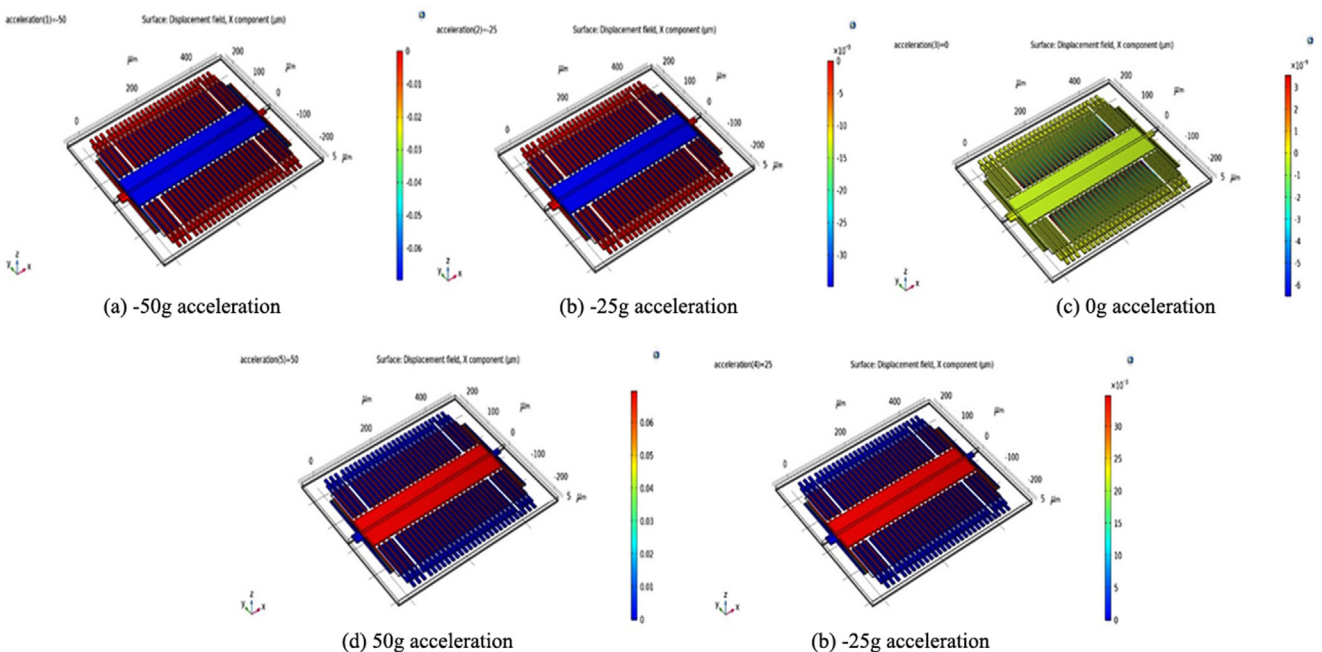


Fig. 3. Simulation result without perforated mass: Displacement field for X component for -50 g (fig. a); -25 g (fig. b); 0 g (fig. c); 25 g (fig. e) 50 g (fig. d) acceleration.

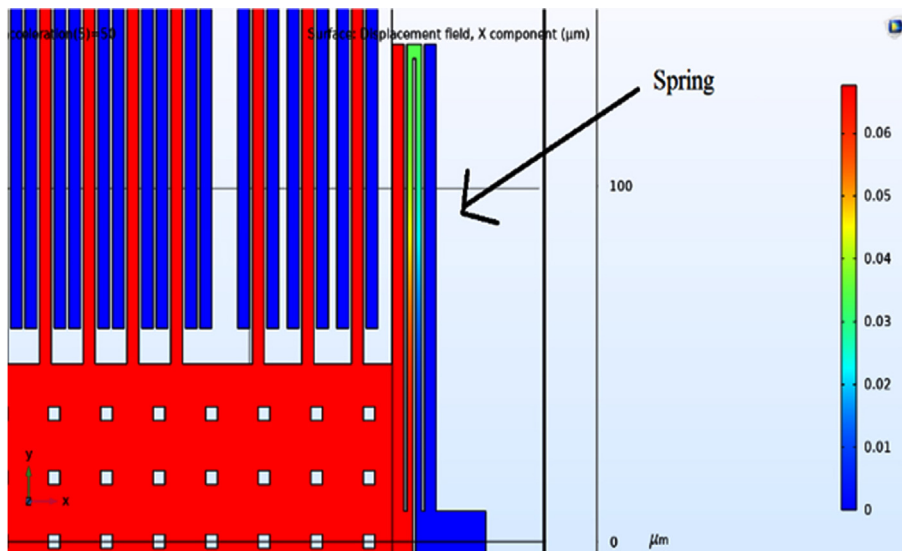


Fig. 4. Varying displacement in spring along its length.

the electrodes, thereby allowing the attached circuitry to process signals more efficiently.

The stationary component of the square wave is modelled in this case using a stationary analysis, which enables the problem to be solved easily. To electrostatic force between electrodes as mentioned earlier, is minimized by setting the bias to 0. It can also be done by dividing a factor of 1000 in the square wave amplitude. This factor is compensated by multiplying it back in the further processing.

The graph between displacement and the acceleration applied is illustrated in Fig. 5. From the graph we can see a linear relationship between the two parameters.

3.3. Sense voltage vs acceleration

The sense voltage and acceleration have a linear relationship. This signal is fed into an amplifier, which was designed on the same substrate as the mechanical system in the actual unit. When the amplitude of the ac signal is changed, the bias is set at -40 to $+40$ dc (Fig. 6).

The accelerometer’s self-test electrodes is designed for the self-testing purpose in factories. In the next study, a bias of 2 V is

applied to the fixed self-test electrodes for the demonstration of self-testing applications.

The electrostatic force generated by the electric field between the fixed and moving electrodes allows the proof mass to shift. As voltage is applied, the displacement of the polysilicon domain is as seen in Fig. 6. It can be seen that the proof mass shifts by around $0.02 \mu\text{m}$. In normal cases we see about $0.06 \mu\text{m}$ displacement. Hence it is optimum for self-testing purposes.

3.4. Comparison and analysis of simulation results

By changing the etch hole size and period in perforated proof mass, the observations are tabulated as follows in Table 2 and Table 3:

3.5. Effect of perforation of proof mass

In this system, the damping properties of air in the narrow gap greatly affects the dynamic performance of the system. The flow of air in the device is necessary. Otherwise, the particles move randomly causing Brownian noise (Due to Brownian motion). In order to reduce this air damping the perforations in proof mass is made.

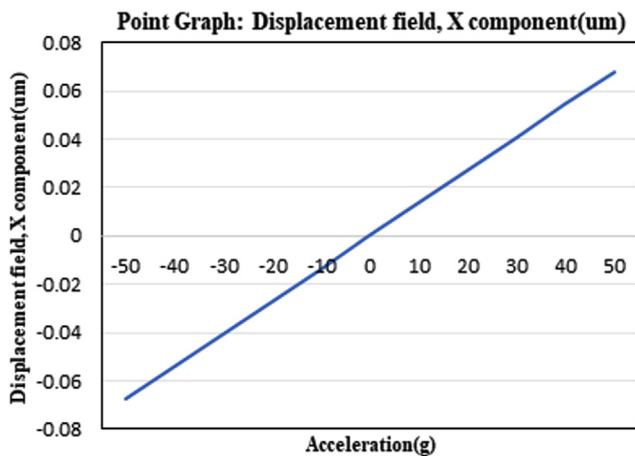


Fig. 5. Point graph displacement field for x component.

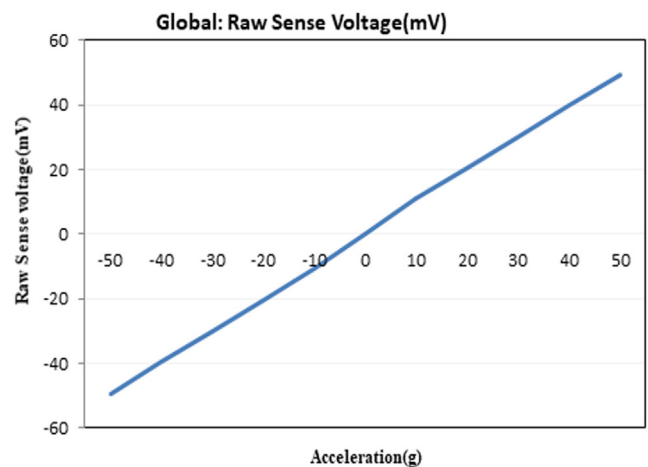
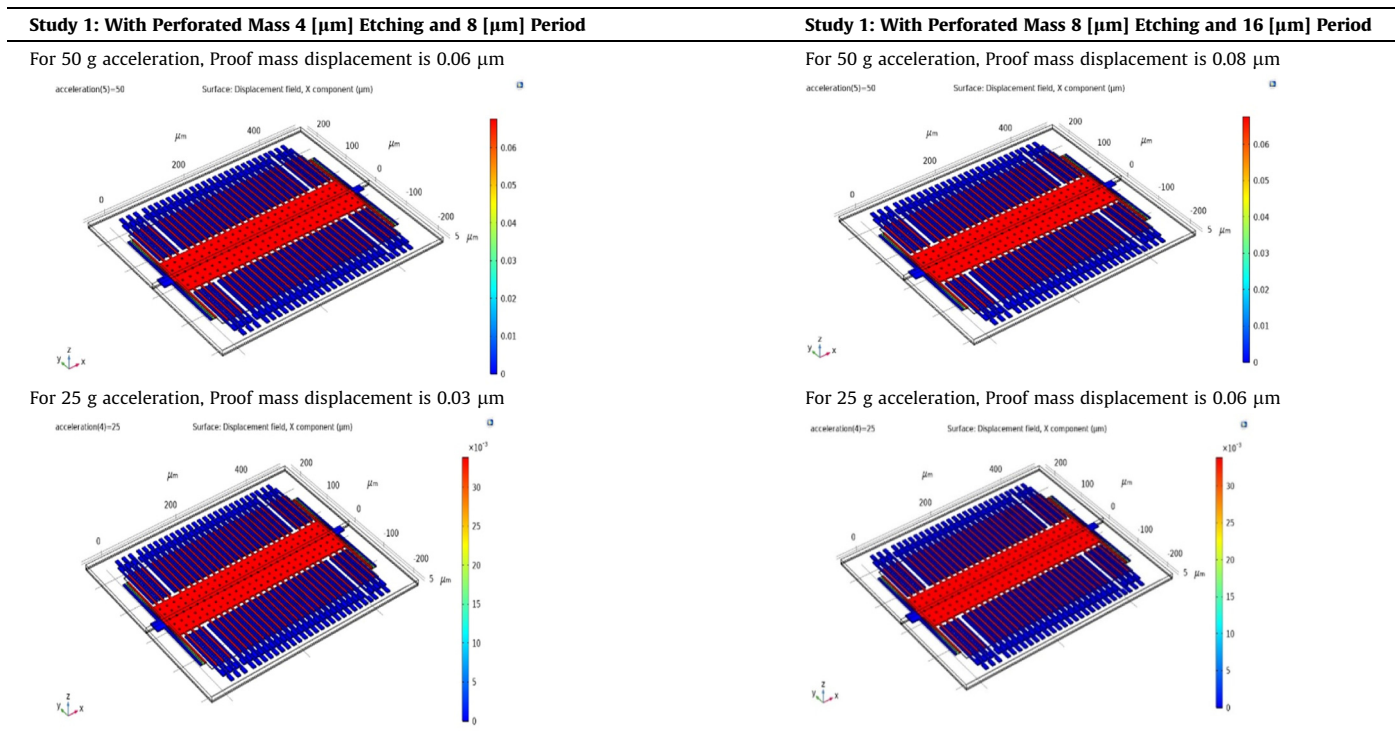


Fig. 6. Raw sense voltage vs Acceleration.

Table 2
Comparison of etch size and period with displacement.

Property	Without perforated mass	With perforated mass	Property
Damping effect Undesired as it affects the dynamic performance	High	Lower	Lowest
Mass M_s Sensing mass	Highest	Reduces	Further reduces
Sensitivity Sensitivity can be defined as the derivative of the output voltage or current with respect to the acceleration	High	Optimal	Low

Table 3
Comparison of etch size and period with displacement.



However, we see that the Displacement sensitivity $S_d \propto M_s$. So, as we use perforations, the mass of the structure is reduced, thereby decreasing the sensitivity. For seismology applications, sensitivity, should be in the order of 10^2 to $mV m^{-1}s^{-2}$ and bandwidth in range between 10^{-2} and 10^2 Hz.

Hence there is a need to maintain an optimum balance between these two parameters (sensitivity and damping) for this application. Therefore, the first study model has better performance, as none of the parameters needs to have a trade-off.

3.5.1. Significant outcome

MEMS accelerometer structures have a large surface area in comparison to their thickness. The efficiency of the system is affected by the damping properties of air in the narrow gap in these squeeze films. Brownian noise is the term for this kind of noise. This is calculated with the below equation.

$$B = \mu \frac{Lh^3}{d^3} \tag{21}$$

Where,
 μ is the Air viscosity ($1.81 \times 10^{-5} Pa.s$); L is the Finger overlap ($10^4 \mu m$); h is the Finger thickness ($2 \mu m$) and d is capacitance

Table 4
Comparison of sensitivities of existing and proposed models.

Parameter/Model	Existing model	Proposed model
Displacement sensitivity	$1.54 \times 10^{-10} m/g$	$1.188 \times 10^{-9} m/g$
Capacitive sensitivity	$7.85 \times 10^{-18} F$	$1.093 \times 10^{-21} F$

Gap ($1 \mu m$). Substituting we find that the noise is about $B = 14.97 ng/\sqrt{Hz}$.

Noise is also significantly diminished. This is because the proof mass has been perforated that reduces the air damping between the moving mass and the fixed electrodes. The sensitivity factor is also improved from the existing model which is as shown in Table 4.

4. Conclusion

This paper provides a system architecture modelling and sensitivity analysis of comb-type MEMS accelerometer for seismic applications. During an earthquake, the a point on the ground keeps changing in terms of its position and experienced forces. Under-water earthquakes are very small and originate at a distant location. So accelerometers with perforated proof-mass are

capable of measuring and monitoring small acceleration signals generated by such earthquakes. Also detecting and continuous monitoring of “pre-seismic” on the ground can be enhanced by this technique. The obtained results indicate that the geometry of structure, such as the width and length of the movable fingers, and that of the spring has significantly improved the acceleration sensitivity. These results suggest that this accelerometer structure may be a good fit for low-frequency applications like seismology. With the help of the studies conducted, the optimized design has been achieved. The developed design can be developed into an integrated system for seismic studies.

Data availability

The raw/processed data required to reproduce these findings cannot be shared at this time as the data also forms part of an ongoing study.

Declaration of Competing Interest

The authors declare that they have no known competing financial interests or personal relationships that could have appeared to influence the work reported in this paper.

Acknowledgment

The authors extend their appreciation to the Deputyship for Research & Innovation, Ministry of Education in Saudi Arabia for funding this research work through the project no. (IFKSURG-2-173).

Availability of data and material

Not applicable.

Code availability

Not provided.

Authors' contributions

The first author had explained the problem, helped in execution of the work and framed the manuscript. The second author was responsible for analysis of results, proof reading the manuscript. The contribution of third, fourth and fifth authors was in modelling and simulation of the proposed accelerometer.

Appendix A. Supplementary data

Supplementary data to this article can be found online at <https://doi.org/10.1016/j.jksus.2023.102560>.

References

- Benmessaoud, M., Nasreddine, M.M., 2013. Optimization of MEMS capacitive accelerometer. *Microsys. Technol.* 19 (5), 713–720.
- Chen, D., Li, G., Wang, J., Chen, J., He, W., Fan, Y., Deng, T., Wang, P., 2013. A micro electrochemical seismic sensor based on MEMS technologies. *Sensor. Actuator A: Physical.* 202, 85–89.
- Gonenli, I.E., Celik-Butler, Z., Butler, D.P., 2011. Surface micromachined MEMS accelerometers on flexible polyimide substrate. *IEEE Sensors J.* 11 (10), 2318–2326.
- Gupta, V., Mukherjee, T., 2000. Layout synthesis of CMOS MEMS accelerometers. *MSM 2000*, 150–153.
- Hou, Y., Jiao, R., Yu, H., 2021. MEMS based geophones and seismometers. *Sensor. Actuat. A: Physical.* 318, 112498.
- Kalaiselvi, S., Sujatha, L., Sundar, R., 2020. Analysis of damping optimization through perforations in proof-mass of SOI capacitive accelerometer. *Analog Integr. Circ. S.* 102 (3), 605–615.
- Kavitha, S., Daniel, R.J., Sumangala, K., 2016. Design and analysis of MEMS comb drive capacitive accelerometer for SHM and seismic applications. *Measurement* 93, 327–339.
- Laine, J., Mougnot, D., 2014. A high-sensitivity MEMS-based accelerometer. *The Leading Edge.* 33 (11), 1234–1242.
- Lynch, J.P., Partridge, K.H., Law, K.H., Kenny, T.W., Kiremidjian, A.S., Carryer, E., 2003. Design of piezoresistive MEMS-based accelerometer for integration with wireless sensing unit for structural monitoring. *J. Aerospace Eng.* 16 (3), 108–114.
- Mistry, K.K., Swamy, K., Sen, S., 2010. Design of an SOI-MEMS high resolution capacitive type single axis accelerometer. *Microsys. Technol.* 16 (12), 2057–2066.
- Mougnot, D., Thorburn, N., 2004. MEMS-based 3D accelerometers for land seismic acquisition: Is it time? *The Leading Edge.* 23 (3), 246–250.
- Peng, C., Chen, Y., Chen, Q., Yang, J., Wang, H., Zhu, X., Xu, Z., Zheng, Y., 2017. A new type of tri-axial accelerometers with high dynamic range MEMS for earthquake early warning. *Comput. Geosci.* 100, 179–187.
- Qu, H., Fang, D., Xie, H., 2008. A monolithic CMOS-MEMS 3-axis accelerometer with a low-noise, low-power dual-chopper amplifier. *IEEE Sensor. J.* 8 (9), 1511–1518.
- Raaja-Bhaskaran, P., Daniel-Rathnam, J., Sumangala, K., 2017. A Simple Analytical Model for MEMS Cantilever Beam Piezoelectric Accelerometer and High Sensitivity Design for SHM (structural health monitoring) Applications. *Transact. Electric. Electron. Mat.* 18 (2), 78–88.
- Sabato, A., Niezrecki, C., Fortino, G., 2016. Wireless MEMS-based accelerometer sensor boards for structural vibration monitoring: a review. *IEEE Sensor. J.* 17 (2), 226–235.
- Scudero, S., Alessandro, A.D., Greco, L., Vitale, G., 2018. MEMS technology in seismology: A short review. In: 2018 Int. Conference Environ. Eng. IEEE, pp. 1–5.
- Tilli, M., Paulasto-Krockel, M., Petzold, M., Theuss, H., Motooka, T., Lindroos, V., eds., 2020. *Handbook of silicon based MEMS Materials and Technologies*. Elsevier.
- Trapani, D., Biasi, N., De Cecco, M., Zonta, D., 2012. Validation of MEMS acceleration measurements for seismic monitoring with LVDT and vision system. 2012 IEEE Workshop on Environmental Energy and Structural Monitoring Systems (EESMS), IEEE, (pp. 104–109).
- Utz, A., Walk, C., Stanitzki, A., Mokhtari, M., Kraft, M., Kokozinski, R., 2018. A high-precision and high-bandwidth MEMS-based capacitive accelerometer. *IEEE Sensor. J.* 18 (16), 6533–6539.
- van Bakel, N., 2013. Silent sensors for stellar echo's and seismic surveys, June.
- Varanis, M., Silva, A., Mereles, A., Pederiva, R., 2018. MEMS accelerometers for mechanical vibrations analysis: A comprehensive review with applications. *J. Braz. Soc. Mech. Sci. Eng.* 40 (11), 1–18.
- Xiong, X., 2005. Built-in self-test and self-repair for capacitive MEMS devices. University of Cincinnati.
- Xu, W., Yang, J., Xie, G., Wang, B., Qu, M., Wang, X., Liu, X., Tang, B., 2017. Design and fabrication of a slanted-beam MEMS accelerometer. *Micromachines.* 8 (3), 77.
- Zhang, H., Wei, X., Ding, Y., Jiang, Z., Ren, J., 2019. A low noise capacitive MEMS accelerometer with anti-spring structure. *Sensor. Actuator. A: Physical.* 296, 79–86.
- Zou, X., Thiruvengatanathan, P., Seshia, A.A., 2014. A seismic-grade resonant MEMS accelerometer. *J. Microelectromech. Sys.* 23 (4), 768–770.